

Enantioanalysis of D-histidine based on its interaction with [5,6]fullerene-C₇₀ and diethyl (1,2-methanofullerene-C₇₀)-71,71-dicarboxylate

Raluca-Ioana Stefan-van Staden*

Received (in Montpellier, France) 20th October 2009, Accepted 1st February 2010

First published as an Advance Article on the web 10th March 2010

DOI: 10.1039/b9nj00583h

Enantioselective, potentiometric membrane electrodes based on [5,6]fullerene-C₇₀ and diethyl (1,2-methanofullerene-C₇₀)-71,71-dicarboxylate were proposed for the enantioanalysis of D-histidine in pharmaceutical compounds. Molecular modelling calculations were performed to support the experimental results. Electronic structures, as well as molecular interactions, have been investigated using Hartree–Fock theory, 3-21G(*) basis set. Stability and feasibility of all the generated structures were supported by their respective energy minima and fundamental frequencies. Molecular modelling calculations were in good agreement with the performances (*e.g.*, response characteristics, enantioselectivity, recovery tests) of the proposed electrodes.

1. Introduction

L-Histidine (L-His) is one of the essential amino acids. An important product of degradation of L-histidine is histamine. L-Histidine is synthesized by mammals from common metabolic intermediates. Young animals and human infants need a constant supply of L-histidine because, like arginine, the rate of L-histidine synthesis in young animals and human infants is inadequate to meet the requirement for growth. A fine scaly erythematous dermatitis is developed in patients on long-term total parental nutrition if no histidine is included in the intravenous nutrient solution.¹ It is necessary for L-histidine to be considered to be at least partially a dietary essential even though L-histidine is not nutritionally important.

L-Histidine is one of the components of the food supplements formulated as capsules, tablets or injections. An enantiopurity test of histidine is needed, as D-histidine does not have any role in the body. D-Histidine can be an impurity in the synthesis of L-histidine.

Capillary electrophoresis,^{2–7} piezoelectric microgravimetry,⁸ fluorimetry,⁹ chromatography, *e.g.*, HPLC,^{10–12} GC-MS¹³ and fluorescence¹⁴ were proposed for the analysis and enantioanalysis of histidine, but they are not always as simple and accurate as electroanalysis. Unfortunately, the existing electroanalytical methods^{15–17} cannot discriminate between L- and D-enantiomers of histidine.

Studies on the electrochemistry of fullerene^{18–20} have opened a new field for their applications in analytical chemistry, namely enantioselective, potentiometric membrane electrodes based on fullerenes. Highly symmetrical molecular cages are of interest to chemists not only because of the nature of their bonding but also because such structures can exhibit unusual reactivity.

In this paper, we propose two enantioselective, potentiometric membrane electrodes based on [5,6]fullerene-C₇₀ and diethyl (1,2-methanofullerene-C₇₀)-71,71-dicarboxylate as chiral selectors. Modified carbon paste was considered for the design of these electrodes due to its high reliability.²¹ Based on that rationale, computational calculations were conducted using *ab initio* molecular orbital theory to corroborate the reliability of the proposed electrodes. Indeed their structural elucidation, electronic properties, energies and related properties could be useful for drug design and pharmacological utility.

2. Experimental details

2.1 Electrode design

The [5,6]fullerene-C₇₀ (**I**) and its derivative diethyl (1,2-methanofullerene-C₇₀)-71,71-dicarboxylate (**II**) were used as chiral selectors for the design of the enantioselective, potentiometric membrane electrodes (EPMEs). Paraffin oil, graphite powder, and the chiral selector (**I** or **II**) were mixed to give the modified carbon paste. A certain quantity of carbon paste free of chiral selector was prepared and it was placed into a plastic pipette tip leaving 3 to 4 mm empty in the top to be filled with the modified carbon paste (Fig. 1). The diameter of the EPMEs was 3 mm. Electric contact was obtained using an Ag/AgCl wire. A solution of 0.1 mol L^{−1} KCl was utilized as the internal solution. The surface of the electrodes was wetted with deionized water and polished with alumina paper (polishing strips 30144-001, Orion) before using them for the experiment. When not in use, the electrode was immersed in a 10^{−3} mol L^{−1} D-histidine (D-His) solution.

2.2 Apparatus

A 663 VA stand (Metrohm, Herisau, Switzerland) connected to a PGSTAT 100 and software (Eco Chemie version 4.9) was used for all potentiometric measurements. A glassy carbon and an Ag/AgCl (0.1 mol L^{−1} KCl) electrode served as counter and reference electrodes, respectively, in the cell.

Laboratory of Electrochemistry and PATLAB Bucharest, National Institute of Research for Electrochemistry and Condensed Matter, 202 Splaiul Independentei Str., 060021, Bucharest, Romania. E-mail: iustinavastaden@yahoo.com; Fax: +40 21 316 3113; Tel: +40 75 150 7779

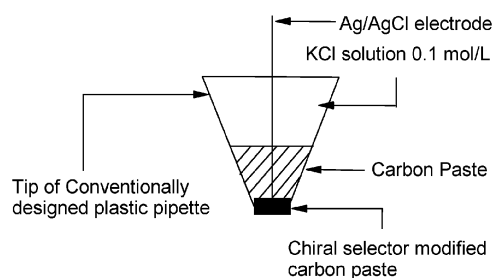


Fig. 1 Design of enantioselective, potentiometric membrane electrode.

2.3 Reagents and materials

[5,6]Fullerene- C_{70} , diethyl (1,2-methanofullerene- C_{70})-71,71-dicarboxylate, L- and D-histidine and paraffin oil were purchased from Fluka (Buchs, Switzerland). Graphite powder (1–2 micron, synthetic) was supplied by Aldrich (Milwaukee, WI, USA). Deionized water from a Modulab system (Continental Water Systems, San Antonio, TX, USA) was used for all solution preparations. The L- and D-His solutions necessary in the characterization of the enantioselective potentiometric membrane electrodes were prepared from standard L- and D-His solutions (10^{-2} mol L^{-1}), respectively, by serial dilutions. All standard and diluted solutions were buffered with phosphate buffer, 0.1 mol L^{-1} (pH 5.30) from Merck (Darmstadt, Germany), in a ratio of 1 : 1 (v/v) buffer:deionized water. Food supplement, energy booster, immunity modulator capsules (containing 0.72 g histidine per capsule) were supplied by Hypo-plus Naturals, South Africa.

2.4 Recommended procedure: direct potentiometry

Direct potentiometry was used for the potential measurement of each standard solution (10^{-10} to 10^{-3} mol L^{-1} , pH 5.30). The electrodes were placed in the stirred standard solutions. Calibration plots were obtained by plotting E (mV) versus pD-His. Unknown concentrations were determined from the corresponding calibration plot.

2.5 Enantiopurity test of the food supplement

Each of ten capsules was placed in a 250 mL volumetric flask and dissolved in a 1 : 1 distilled water:buffer (pH = 5.4) solution. The unknown concentration was determined using the direct potentiometric method.

2.6 Molecular modelling calculations

The structures [5,6]fullerene- C_{70} (**1**), diethyl (1,2-methanofullerene- C_{70})-71,71-dicarboxylate (**2**), D-histidine (**3**), complex between [5,6]fullerene- C_{70} and D-His (**4**), and complex between diethyl (1,2-methanofullerene- C_{70})-71,71-dicarboxylate and

D-His (**5**), were generated for the prediction of chiral interaction between fullerenes as chiral selectors and D-histidine.

The electronic structures with lower energy conformation and derived properties of all the compounds **1** to **5** were obtained by *ab initio* theory. However, molecular calculations started with the fully optimized semiempirical PM3 level of theory, followed by the minimal STO-3G basic set Hartree-Fock model. The resulting wavefunction, Hessian matrix and the geometry of the molecules obtained were used to perform a final calculation with the split-valence basis set 3-21G(*). The asterisk means that “d” polarization functions were added for carbon, oxygen and nitrogen atoms.

To obtain a realistic and detailed picture of chiral interaction, the following physicochemical parameters were used: total energy, highest occupied MO (HOMO), lowest unoccupied MO (LUMO), dipole moment (μ), atomic charge, bond length and hardness (η). Fundamental frequencies at the semiempirical level (PM3) of all the molecules were calculated.

Computer calculations were carried out on a Pentium 4 (3.2 GHz) based computer. The software utilized was Spartan’04 Windows²² and CorelDRAW 12.

3. Results and discussion

3.1 Response of the electrodes

The response characteristics exhibited by the proposed electrodes towards the detection of D-His are summarized in Table 1. For both calibration plots, the potentiometric membrane electrodes showed linear near-Nernstian responses for D-histidine, with correlation coefficients for the equations of calibration of 0.9999, while the plots for L-histidine showed a non-Nernstian response.

The response times for the diethyl (1,2 methanofullerene- C_{70})-70,70-dicarboxylate-based electrode was 30 s. The response time for the electrode based on [5,6]fullerene- C_{70} was 25 s for concentrations between 10^{-10} and 10^{-8} mol L^{-1} and 10 s for concentrations higher than 10^{-8} mol L^{-1} . All electrodes displayed good stability and reproducibility over the test, as shown by the relative standard deviation values (RDS < 1.0%).

3.2 Mechanism of the potential development

The mechanism of the potential development is based on the formation of a complex between D-histidine and the chiral selector, [5,6]fullerene- C_{70} or (1,2 methanofullerene- C_{70})-70,70-dicarboxylate. The molecular modelling calculations support the new theory of potential development: the higher the stability of the complex the higher the slope of the electrode.²¹

Table 1 The response characteristics of the enantioselective, potentiometric, membrane electrodes based on C_{70} fullerene and its derivative^a

EPME based on	Slope (mV/decade of conc.)	Intercept, E° (mV)	Linear conc. range (mol L^{-1})	Detection limit (mol L^{-1})
I	54.4	705.4	10^{-10} – 10^{-5}	1.1×10^{-13}
II	56.5	680.6	10^{-11} – 10^{-5}	9.2×10^{-13}

^a All measurements were made at room temperature; all values are the average of ten determinations.

3.2.1 Computations and electronic structure. The molecular modelling and calculations were performed in order to prove the interaction between D-histidine and chiral selector. Unfortunately, at this stage it was not possible to show why the sensors were enantioselective using the theoretical calculations and modelling. To corroborate the experimental results of the proposed fullerene electrodes for the enantioanalysis of D-His, computational calculations were conducted: lower energy

conformation and physicochemical properties were calculated for chiral selectors **1** and **2**, separately and along with the analyte. Computer-generated lower energy electronic structures are presented in Fig. 2 and 3.

The X-ray structure of fullerene²³ shows two different bond lengths (1.389 Å and 1.432 Å) for bonds between two hexagons, and for those between a hexagon and a pentagon, referred to as [6,6] and [6,5], respectively (Fig. 2A). Both numbers lie

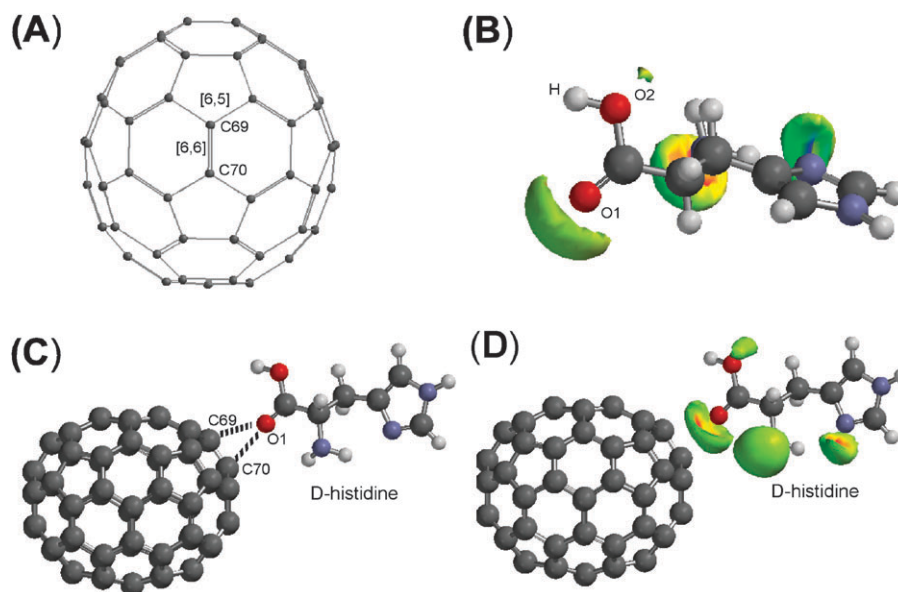


Fig. 2 The electronic and molecular structures obtained from theoretical calculations. (A) [5,6]Fullerene-C₇₀, showing two binding types. (B) Electrostatic potential map of D-histidine showing the lone pair on nitrogen and oxygen atoms. (C) The complex formed between C₇₀ fullerene and D-histidine, signifying intermolecular interaction. (D) Electrostatic potential map of the complex formed between C₇₀ fullerene and D-histidine.

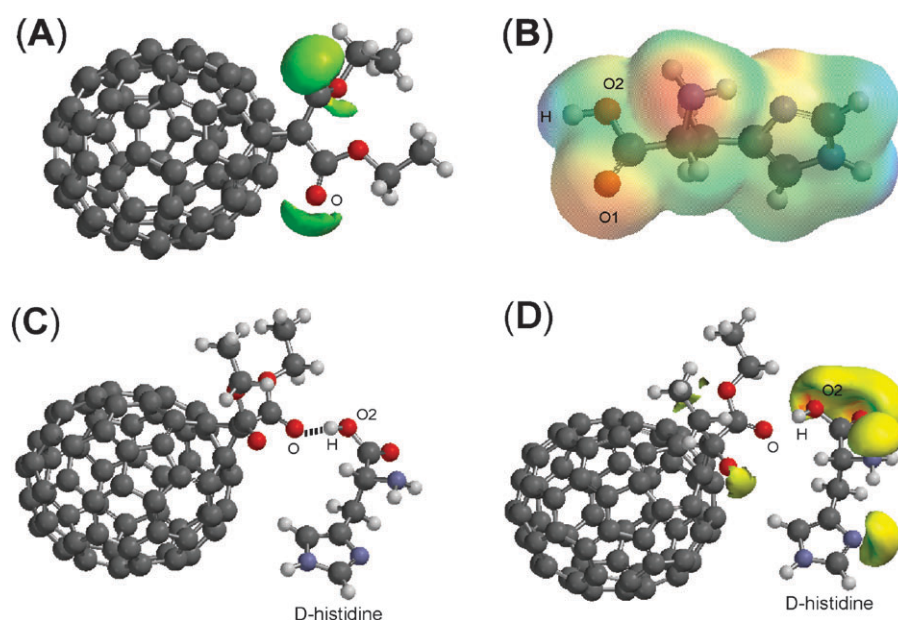


Fig. 3 The lower energy electronic and molecular structures generated from theoretical calculations. (A) Electrostatic potential map of diethyl (1,2-methanofullerene-C₇₀)-71,71-dicarboxylate, showing lone pairs on oxygen atoms. (B) Electron density encoded with potential map of D-histidine molecule, presenting overall molecular size and shape; red is electronegative and blue is electropositive. (C) The complex formed between fullerene derivative and D-histidine, showing hydrogen bonding. (D) Electrostatic potential map of the complex between fullerene derivative and D-histidine, showing lone pairs on oxygen and nitrogen atoms, considering that the electrostatic potential is not located on O oxygen atom.

Table 2 Calculated most representative bond lengths of chiral selectors separately and with D-histidine

Bond	Bond length (Å)			
	1	2	4	5
[6,6]	1.370	1.576	1.370	1.552
[6,5]	1.452	1.488	1.452	1.495

between standard sp^2-sp^2 (1.33 Å) and sp^3-sp^3 (1.54 Å) bond lengths. Table 2 displays the most representative bond lengths [6,6] and [6,5] obtained in these computations. It is worthwhile to mention at this point that computed bond lengths always reasonably reproduce some experimental differences. Thus, the bond lengths are in favour of the accuracy of the fullerene geometry obtained. Significantly, the [6,6] bond length in the compounds **2** (fullerene derivative) and **5** (complex between fullerene derivative and D-His) show the single bond character due to the presence of bridging carbon C71 with the fullerene case, which changes the corresponding sp^2-sp^2 bond length of the [6,6] bond of the compound **1** to sp^3-sp^3 in the compounds **2** and **5**.

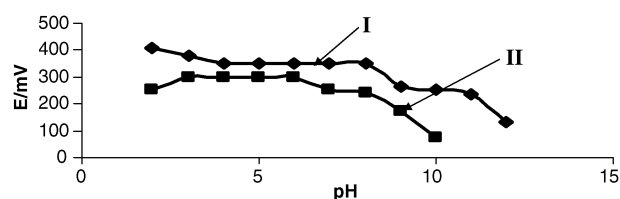
The distances from the C69 and C70 carbon atoms of C_{70} fullerene to the D-His carboxylic oxygen observed are 3.2 Å and 3.3 Å, respectively (Fig. 3C). This molecular interaction is due to the availability of lone pairs on D-His carboxylic oxygen, which interact with the π electrons of the fullerene case. On the other hand, distance from carboxylate oxygen of fullerene derivative to the carboxylic hydrogen of D-His is 1.7 Å (Fig. 3C), which indicates the occurrence of a hydrogen bonding interaction. Therefore it is concluded that there is a strong interaction between C_{70} derivative and D-His evidenced by the hydrogen bonding distance. This is in agreement with experimental results, as the electrode based on the fullerene derivative had a greater slope than the one based on C_{70} .

Some molecular properties changed from structure **1** (C_{70}) when compared with **4** (complex between C_{70} and D-His) as a consequence of different electronic distribution. As revealed in Table 3, the C69 and C70 carbon atoms of compound **1** decreased in electronegativity and increased in electropositivity, respectively, when compared with compound **4**. The interaction of C_{70} as a chiral selector with the D-His (Fig. 2C) during the enantiopurity assay is in agreement with the changes in atomic charges, as the polarization of atoms C69 and C70 from **1** to structure **4**. Which signifies that these atoms could share their charge with carboxylic O1 oxygen of D-His, which subsequently shows the increase in its electronegativity from compound **3** to compound **4**. The localization of electrostatic potential was due to the D-His molecule only; C_{70} fullerene did not participate in the formation of electrostatic

potential as shown in Fig. 2D. Fig. 2B presents the electrostatic potential map of the free D-His molecule, signifying the reactive oxygen (O1) atom with its large electrostatic potential. Thus, modification of charges and electrostatic potential indicate the existence of a very weak interaction between C_{70} and D-histidine.

The oxygen (O) of the fullerene derivative (**2**) increased its electronegativity and decreased its electrostatic potential when compared with compound **5**, as revealed in the electronegativity shown in Table 3 and electrostatic potential shown in Fig. 3A and D. It is observed that the hydrogen (H) and O2 atom of the carboxylic group of D-His increased its electropositivity and decreased its electronegativity, respectively, when comparing structure **3** with **5**. As well as this, the electrostatic potential of O2 increased when comparing Fig. 2B with 3D. It is clear that the O of the fullerene derivative, due to the lack of natural charges, accepts charges from the H of the carboxylic acid of D-His and thus leaves the H atom more electropositive in **5**, causing the involvement of a hydrogen bonding interaction. The localization of electrostatic potential changed in good agreement with electronic density of atoms (decrease in electronegativity of atoms increases the electrostatic potential). It is worthwhile to mention here that the presence of the proton acceptor oxygen (O) in the fullerene derivative **2** and the proton donor oxygen (O2) in D-histidine **3**, results in a hydrogen bonding interaction. Fig. 4B shows the density encoded with the potential map of the free D-His molecule, pointing to the electronegativity of the oxygen atoms with red colour and the electropositivity of the H atoms with blue colour. The modification of charges and electrostatic potential are in favour of the strong hydrogen bonding interaction between the fullerene derivative and D-His (Fig. 3C).

The common feature of the interaction of C_{70} fullerene (**1**) and its derivative (**2**) with D-His is the increased total energy of compounds **4** and **5**, as compared to **1** and **2**, respectively (Table 4). It has been observed experimentally that fullerene and its derivative undergo chiral interaction with D-His, thus it

**Fig. 4** The influence of pH on the response of the enantioselective potentiometric membrane electrodes (D-His = 10^{-5} mol L $^{-1}$); for electrodes based on **I** ([5,6]fullerene- C_{70}) and **II** (diethyl (1,2-methanofullerene- C_{70})-71,71-dicarboxylate).**Table 3** Calculated selected atomic charges of all the considered structures involved in the interaction of D-His with fullerene as a chiral selector

Atom	Charge ^a		Atom	Charge ^a		Atom	Charge ^a		
	1	4		2	5		3	4	5
C69	-0.012	-0.005	O	-0.616	-0.641	O1	-0.625	-0.643	—
C70	0.008	0.022				O2	-0.768	—	-0.761
						H	0.489	—	0.491

^a Natural charges in electrons.

is possible to gain 542.5 hartrees, corresponding to the addition of D-His molecule. This is a common situation because there are reported Hartree–Fock energies for atoms where it has been observed that energy increases when the number of atoms increases.²⁴

2.4 kcal mol⁻¹ is the value of the binding energy of C₇₀, with the D-His molecule calculated as the energy difference between the total energy of **4** and the sum of the total energies of **1** and **3**. Similarly, 30.9 kcal mol⁻¹ is the value of the binding energy of the C₇₀ derivative, with D-His calculated as the energy difference between the total energy of **5** and the sum of the total energies of **2** and **3**. Accordingly, the interaction between the fullerene derivative and the analyte D-His is stronger than C₇₀ and D-histidine.

The HOMOs of compounds **1–5** have lower values for energy than the LUMOs. Accordingly, the Fukui postulate²⁵ is fulfilled, since electrons in orbital with higher energy are more susceptible to receive the nucleophilic species, whereas the electrons in orbitals with lower energy are more susceptible to receive the electrophilic species.

Dipole moments (μ), as revealed from Table 4, for the structures **4** and **5** are greater than those for the structures **1** and **2**, respectively, because the addition of polar D-His modifies the charge distribution of the former compounds. It is believed that the double bonds of C₇₀ fullerene (**1**) are polarized in opposite directions, which nullifies the electronic density, giving it a zero dipole moment. Compound **2** has a higher dipole moment than **1**, as the presence of a methano dicarboxylate group causes polarization in the former. Hence, because of its polarization, compound **2** is more reactive with D-His than compound **1**.

It is observed that the hardness values, $\eta = -(\epsilon_{\text{HOMO}} - \epsilon_{\text{LUMO}})/2$,²⁶ indicated that the compounds **1** and **2** decreased their hardness on interaction with D-His. Compound **5** is softer than **4**, which clearly indicates the involvement of a strong force of intermolecular interaction in the former. This property supports the fact that, according to Pearson,²⁶ soft molecules are more reactive than hard molecules. Thus, the hardness values support the experimental results, which indicate the better reactivity of the C₇₀ derivative compared with C₇₀.

Table 4 summarizes the common properties of all the compounds involved in the chiral interaction of fullerene with D-His: total energy, frontier orbital energies (HOMO and LUMO), hardness and dipole moment.

Computing their harmonic normal modes of vibration allowed us to assess the structural stability and feasibility of all the molecules **1** to **5**. The lowest-lying normal mode of vibration for each of the molecules **1**, **2**, **3**, **4** and **5** are 224.25, 25.97, 40.91, 3.68 and 9.73 cm⁻¹, respectively. The absence of imaginary (negative) frequencies indicates that the structures

of all the molecules are local minima on the corresponding potential energy surfaces.

The total energy, frontier orbital energies, hardness, dipole moment, atomic charges, electrostatic potential, intermolecular distances and bond length parameters were helpful to provide a logical explanation of the nature of the interaction between fullerene and D-His. Based on the computational modelling calculations, diethyl (1,2-methanofullerene-C₇₀)-71,71-dicarboxylate shows the strongest hydrogen bonding with D-His, thus the complex formed is more stable than the one of C₇₀, which is in good agreement with our experimental results: the highest slope for the electrode was obtained when the fullerene-based, enantioselective, potentiometric membrane electrode was used.

3.3 Effect of pH on the response of electrodes

The influence of pH on the response of the EPMEs was checked by recording the emf of the cell for solutions containing 10⁻⁵ mol L⁻¹ D-His at different pH values (pH 1–12). These solutions were prepared by adding very small volumes of HCl/NaOH solution (0.1 mol L⁻¹ or 1 mol L⁻¹ of each) to a D-His solution.

The plots of E (mV) versus pH (Fig. 4) indicate that the response of the electrodes does not depend upon the pH in the following range: 4.0–8.0 (**I**) 2.0–7.0 (**II**).

3.4 Selectivity of the electrode

The selectivity of the potentiometric membrane electrode was checked using the mixed solutions method. The concentrations of interfering ions and D-His were 10⁻⁴ and 10⁻⁵ mol L⁻¹, respectively. The values obtained for L-His, PVP, creatine and creatinine demonstrated the enantioselectivity and selectivity properties of the proposed EPMEs for the assay of D-His (Table 5). Unfortunately, the molecular modelling calculations to date cannot explain the enantioselectivity of the proposed electrodes; some of the reasons are: the calculated values for L- and D-enantiomers are the same, and the modelling is done “in vacuum”. Experimentally, this is demonstrated by the values obtained for the potentiometric selectivity coefficients which reflect that the chiral selector preferred only one of the enantiomers – namely D-histidine. In 1981, Hulanicki and Lewenstam²⁷ showed that the selectivity of these electrodes is a measure of the competitive equilibria that occurs at the membrane–solution interface between the ions extracted from the bulk solution (main ion and interfering ions) and the ligand. Accordingly, the complexes formed by D-histidine with the fullerenes are more stable than those formed by L-histidine with the same ligands – this being proved experimentally by the values obtained for the potentiometric selectivity coefficients.

Table 4 Values of the electronic and molecular properties of all the compounds involved in the chiral interaction

Compound	Energy (hartree)	HOMO (eV)	LUMO (eV)	Hardness, η (eV)	Dipole moment, μ (debye)
1	-2635.63650	-7.97	-0.84	3.565	0.00
2	-3202.82157	-7.57	-0.61	3.480	5.41
3	-542.472821	-8.94	4.90	6.920	5.76
4	-3178.11312	-7.75	-0.63	3.560	7.54
5	-3745.24514	-7.90	-1.11	3.395	10.71

Table 5 Potentiometric selectivity coefficients (K_{pot}) of the electrodes used for assay of D-histidine^a

Interfering species (J)	EPME based on	
	I	II
L-His	$\ll 1 \times 10^{-4}$	2.30×10^{-3}
PVP	4.5×10^{-3}	2.00×10^{-3}
Creatine	1.3×10^{-3}	3.24×10^{-4}
Creatinine	9.4×10^{-4}	2.95×10^{-3}

^a All measurements were made at room temperature; all values are the average of ten determinations.

Table 6 Recovery of D-histidine (%) in the presence of L-histidine^a

L:D mol/mol	EPMEs based on	
	I	II
2:1	99.93 ± 0.02	99.95 ± 0.02
1:1	99.96 ± 0.02	99.93 ± 0.02
1:2	99.95 ± 0.01	99.97 ± 0.01
1:4	99.97 ± 0.02	99.96 ± 0.02
1:9	99.96 ± 0.02	99.96 ± 0.02

^a All measurements were made at room temperature; all values are the average of ten determinations.

3.5 Analytical applications

The proposed enantioselective, potentiometric membrane electrodes proved to be useful for the determination of enantiopurity of histidine raw material and for performing the enantiopurity test of pharmaceutical compounds containing histidine. The assays of D-His were conducted using different ratios between D- and L-His.

The good recovery values obtained for the determination of D-enantiomer in the presence of L-enantiomer (Table 6) demonstrated the suitability of the proposed enantioselective, potentiometric membrane electrodes for testing the enantiopurity of histidine raw material.

The average recoveries of D-His in the capsules were $2.58 \pm 0.82\%$ ($N = 10$) (I) and $2.67 \pm 0.14\%$ ($N = 10$) (II), respectively for the two electrodes. *t*-Test and *F*-test were also performed at 95% confidence level for the methods proposed for the enantioanalysis of D-histidine. The value obtained for $t = 1.950$ was less than the one tabulated, $t_{\text{tabulated}} = 2.262$, meaning that there is no significant difference between the two methods at 95% confidence level. The value obtained for $F = 1.25$ is less than the tabulated value, $F_{\text{tabulated}} = 3.18$, meaning that there is no significant difference in the precision of the two methods.

4. Conclusions

This paper describes enantioselective, potentiometric membrane electrodes designed using [5,6]fullerene- C_{70} and diethyl (1,2-methanofullerene- C_{70})-71,71-dicarboxylate as chiral selectors in the enantioanalysis of histidine. The electrodes can be successfully used for the assay of D-histidine in the presence of L-histidine. The enantioselectivity is good for both of the two proposed electrodes; the best being recorded when diethyl (1,2-methanofullerene- C_{70})-71,71-dicarboxylate is used as a

chiral selector. The simple, fast and reproducible construction of the electrode assures reliable response characteristics. The good enantioselectivity of the designed electrodes allows us to perform the enantiopurity assay upon raw D-His material in addition to capsule samples. To verify the experimental results related to the molecular interaction between fullerenes and D-His, computational modelling was carried out using *ab initio* molecular orbital theory. Based on the results obtained from theoretical calculations, it was concluded that the slopes of the electrodes are endowed by the molecular interaction implicated between C_{70} fullerene as well as diethyl (1,2-methanofullerene- C_{70})-71,71-dicarboxylate with D-His. Thus, we proved experimentally as well as theoretically that the strongest interaction is taking place between diethyl (1,2-methanofullerene- C_{70})-71,71-dicarboxylate as a chiral selector and D-histidine through hydrogen bonding. This is reflected in a greater slope of the enantioselective, potentiometric membrane electrode based on the C_{70} fullerene derivative. Unfortunately, at this stage the enantioselectivity was only proven by the experiments and not by the values obtained using computational modelling.

Acknowledgements

The author is grateful to Nucleus Project No. PN 07-33 01 04, contract no. 34N/2009.

References

- 1 C. I. Harris and G. Milne, *Br. J. Nutr.*, 1981, **45**, 423–445.
- 2 P. Tuma, E. Samcova and P. Balynova, *J. Chromatogr., B: Anal. Technol. Biomed. Life Sci.*, 2005, **821**, 53–59.
- 3 S. Zhao and Y. M. Liu, *Anal. Chim. Acta*, 2001, **426**, 65–70.
- 4 M. Jalali-Heravi, Y. Shen, M. Hassanisadi and M. G. Khaledi, *Electrophoresis*, 2005, **26**, 1874–1885.
- 5 K. Tsukagoshi, K. Nakahama and R. Nakajima, *Anal. Chem.*, 2004, **76**, 4410–4415.
- 6 N. V. Komarova, J. S. Kamentsev, A. P. Solomonova and R. M. Anufrieva, *J. Chromatogr., B: Anal. Technol. Biomed. Life Sci.*, 2004, **800**, 135–143.
- 7 L. Y. Zhang and M. X. Sun, *J. Chromatogr., A*, 2004, **1040**, 133–140.
- 8 Z. H. Zhang, H. P. Liao, H. Li, L. H. Nie and S. Z. Yao, *Anal. Biochem.*, 2005, **336**, 108–116.
- 9 X. Li, H. Ma, S. Dong, X. Duan and S. Liang, *Talanta*, 2004, **62**, 367–371.
- 10 S. W. Hovorka, T. D. Williams and C. Schoneich, *Anal. Biochem.*, 2002, **300**, 206–211.
- 11 V. Lozanov, S. Petrov and V. Mitev, *J. Chromatogr., A*, 2004, **1025**, 201–208.
- 12 J. L. Bernal, M. J. Nozal, L. Toribio, J. C. Diego and A. Ruiz, *J. Sep. Sci.*, 2005, **28**, 1039–1047.
- 13 A. Namera, M. Yashiki, M. Nishidi and T. Kojima, *J. Chromatogr., B: Anal. Technol. Biomed. Life Sci.*, 2002, **776**, 49–55.
- 14 X. H. Li, H. M. Ma, L. H. Nie, M. Sun and S. X. Xiong, *Anal. Chim. Acta*, 2004, **515**, 255–260.
- 15 L. Z. Wang and X. L. Zhang, *Chin. J. Anal. Chem.*, 1993, **21**, 569–575.
- 16 J. C. Moreira and A. C. Fogg, *Analyst*, 1990, **115**, 41–43.
- 17 X. L. Zhang, C. S. Ma and L. A. Deng, *Chin. J. Anal. Chem.*, 1995, **6**, 783–790.
- 18 D. E. Cliffel and A. J. Bard, *J. Phys. Chem.*, 1994, **98**, 8140–8143.
- 19 J. Chlistunoff, D. Cliffel and A. J. Bard, *Thin Solid Films*, 1995, **257**, 166–184.
- 20 S.-Z. Kang, S.-L. Xu, H.-M. Zhang, L.-B. Gan, C. Wang, L.-J. Wan and C.-L. Bai, *Surf. Sci.*, 2003, **536**, L408–L414.

-
- 21 R. I. Stefan, J. F. van Staden and H. Y. Aboul-Enein, *Electrochemical Sensors in Bioanalysis*, Marcel Dekker, New York, 2001.
- 22 *Spartan'04 Version 1.0.3*, Wavefunction, Inc. 18401 Von Karman Ave., Suite 370, Irvine, CA 92612 USA.
- 23 W. Kratschmer, L. D. Lamb, K. Fostiropoulos and D. R. Huffman, *Nature*, 1990, **347**, 354–358.
- 24 S. R. Gadre, S. B. Sears, S. J. Chakravorty and R. D. Bengale, *Phys. Rev.*, 1985, **A32**, 2602–2606.
- 25 K. Fukui, *Science*, 1982, **218**, 747–754.
- 26 R. G. Pearson, *J. Chem. Educ.*, 1987, **64**, 561–567.
- 27 A. Hulanicki and A. Lewenstam, *Anal. Chem.*, 1981, **53**, 1401–1405.